THE EFFECT OF SHORT CYCLING AND FAN DELAY ON THE EFFICIENCY OF A MODIFIED RESIDENTIAL HEAT PUMP

W.J. Mulroy
ASHRAE Member

ABSTRACT

The object of this study was to determine if the use of a cycling controller would improve the efficiency of a residential air conditioner or heat pump. Cyclic tests were performed on a capillary tube heat pump in three configurations: as manufactured, as modified to simulate a non-bleed expansion valve unit by operation of a valve in the liquid line, and as modified to simulate an air conditioner by elimination of the accumulator. The two modifications, the liquid line valve installation and accumulator removal, were found to greatly improve the cyclic performance to about equal levels; however, some cyclic losses remained. It was concluded that any control strategy that resulted in shortened on-cycle run times would reduce cyclic efficiency for all designs tested. It was further concluded, based in part on the work of others, that fan delay is an undesirable control strategy for units that have the indoor air handler and coil installed within the conditioned space.

INTRODUCTION

Cycling controllers, sometimes called duty cyclers or short cyclers, are additions to the control circuit that are intended to increase the seasonal efficiency of an air conditioner or heat pump by causing the compressor to cycle on and off more rapidly than it would under the control of the room thermostat supplied by the manufacturer. Since the term duty cycler is also used to describe devices that temporarily shed load in commercial applications, which have their electricity rate set by peak demands, this term will not be used in this report to describe the residential devices that were the subject of this study.

Cycling controllers have become popular as a result of the availability of relatively low cost, solid state, timing, temperature sensing, and logic circuits. A typical strategy for a purely timer-based controller might be, when compressor operation is called for by the room thermostat, to shut the compressor off after seven minutes of operation and then turn it on after an additional five minutes, allowing this cycling pattern to continue but leaving the indoor fan running until the room thermostat is satisfied. A typical temperature-based cycling controller might substitute for the above timer criteria compressor shutoff at a supply air temperature 20 F (11°C) below and compressor cut-on at a supply air temperature of 5 F (3°C) below the return air temperature in the cooling mode. These two basic control concepts can be intermingled. Indoor fan control or delay is frequently provided. An override is generally provided to modify the cycling strategy or to allow full-load operation if the original strategy does not provide sufficient capacity to meet the building load. It is important to note that the DOE/NBS ratings of SEER and HSPF do not reflect efficiency differences for different control strategies; rather, these ratings are based on the cycling strategy of a typical thermostat.

Because of the many manufacturers and many possible control strategies for these devices, it was decided not to test specific devices but rather to analyze typical central air conditioner and heat pump cyclic performance to identify possible control strategies that would

William J. Mulroy is a Mechanical Engineer in the Building Equipment Division of the Center for Building Technology at the National Bureau of Standards, Gaithersburg, Maryland.

result in energy savings. To provide the needed data, laboratory tests were performed on a split unit, fixed-orifice expansion-device heat pump modified to exhibit cyclic performance typical of several other classes of residential equipment. The primary modifications used for some of these tests were removal of the accumulator to simulate an air conditioner and use of a pneumatically operated ball valve in the liquid line to simulate an expansion valve without a bleed port.

TEST SPECIMEN AND FACILITY

A nominal three ton, R22, split system, air-to-air unitary heat pump was used in this investigation. The unit was equipped with a crankcase heater that was automatically energized during all "off" cycles. The outdoor unit contained the compressor, outdoor coil, fan defrost controller, and associated equipment. The indoor and outdoor sections of the heat pump were installed in separate but adjoining environmental chambers.

This heat pump had been modified, as part of a previous study relating refrigerant migration to cyclic loss (Mulroy and Didion 1985), by the installation of pneumatically operated ball valves capable of isolating system components (liquid line, suction line, evaporator, condenser, compressor, and accumulator). One of these valves (in the liquid line) was used to simulate operation with a thermostatic expansion valve without a bleed port (i.e., no refrigeration migration during the off-cycle) and the remaining valves were deactivated.

As part of another study, this heat pump had been modified to use interchangeable orifice elements (short, small diameter capillary tubes, 0.5 inches in length) instead of the original capillary tubes. Orifice elements found to give optimum steady-state performance with refrigerant 22 using charging criteria typical of commercial practice were used in this study.

Different orifice sizes were not considered in this study because it was felt that the amount of charge would be the primary variable affecting cyclic performance of units that allow off cycle migration. That is, orifice size would not have an effect on the amount of off cycle migration or on the return rate of the refrigerant to its steady-state locations in the system upon start-up. Orifice sizing would only affect cycling performance as it would affect total charge and charge distribution at steady-state, which variables were studied by varying charge as described below.

Two additional unit modifications were made for some tests in this study. First, the total unit charge was reduced by approximately two pounds by reducing the liquid line volume. This was accomplished by reducing the liquid line diameter (0.5 inch to 0.37 inch O.D.), by eliminating several valves, the liquid line filter drier, and a turbine flowmeter (which would have normally been used in steady-state testing for measurement of refrigerant side capacity), and by removing bypass loops needed for maintaining the correct direction of flow through the tubine meter during reverse cycle operation. Second, to simulate an air conditioner, the accumulator was removed from the system and replaced by a straight section of tubing.

Unit capacity was measured using the indoor air enthalpy method. An airflow-rate measuring apparatus was connected to an insulated duct attached to the discharge side of the indoor section of the unit. This apparatus consisted of a receiving chamber and a discharge chamber separated by a partition containing a nozzle. An exhaust fan was attached to the duct leaving the discharge chamber so that the static pressure of the air leaving the indoor section could be adjusted to give airflow rates consistent with the manufacturer's performance data.

Capacitance type pressure transducers accurate to within 0.2% of the reading were used to measure static pressure across the nozzle, and the pressure difference was obtained by a pitot tube placed at the nozzle exit.

A 30-junction thermopile was used to measure the air temperature difference entering and leaving the indoor section of the heat pump. One side of the thermopile was placed in the entering duct, while the other was placed in the insulated discharge duct leading to the receiving chamber of the airflow-measuring apparatus. The junctions of the thermopile were spaced at centers of equal area across the inlet and discharge ducts.

The relative humidity of the air entering the indoor unit was measured by a motorized psychrometer.

No secondary test method was used, since no adequate secondary test method for cyclic operation has been developed and because the measured steady-state performance was to be used only for normalization of cyclic data and to verify comparability of initial conditions between tests.

Watt-hour meters were installed to measure the electrical energy consumption of the compressor and outdoor fan, and the indoor fan and control circuit during steady-state operation. An analog watt meter was also used to measure the electrical energy consumption of the compressor and outdoor fan during steady-state and cyclic operation, since the discrete counts of fractional watt hour meter disc revolution did not provide adequate resolution during rapid data scan rate cycling tests. Crankcase heater power was measured but was not used in the reported calculations.

The dry-bulb and dew-point temperatures in both the indoor and outdoor environmental chambers were continuously recorded. The average temperature of the air entering the outdoor unit was measured using four thermocouples connected in parallel. In addition to the preceeding instrumentation, thermocouples and pressure transducers were installed at various locations and temperatures and pressures were recorded to provide additional information on the performance of the unit and as a check on consistent operation.

Electric resistance heaters, which cycled "on" or "off" as the unit cycled, were installed in the appropriate test chamber to stabilize the load on the test chamber's environmental control systems.

All data were recorded using an automatic data acquisition and control system equipped with a 5 1/2 digit digital voltmeter. The fastest scan rate used during transient testing was readings of a set of 14 data items at intervals of approximately 2.5 seconds.

TEST PROCEDURE

The test procedures followed were those of the current Department of Energy (DOE) test procedure (DOE 1979) with the exception that continuous indoor fan operation was employed. The primary reason for this deviation was that most short cycling devices employ fan delay or continuous fan operation until the thermostat is satisfied. A secondary reason is that continuous indoor fan operation has been found to provide more repeatable test data than cyclic fan operation and has, for this reason, been incorporated in ASHRAE Standard 116-83 (1983).

All cooling mode tests were performed at the DOE dry coil 82 F (27°C) outdoor ambient air test condition and all heating mode tests were performed at the DOE 47 F (8°C) ambient air test condition.

No wet coil cyclic cooling tests were performed. No credance was given to the argument that there is value during cooling operation in reevaporating condensed water by fan delay during the off-cycle to trade reduced latent capacity for increased sensible capacity. That is, the traditional concept was followed of treating latent and sensible capacity as being of equal value and the reported total capacity being equal to their unweighted sum.

The general test procedure followed within the guidelines of DOE (1979) was to perform a steady-state test for a 40-minute data period, which was immediately followed by two sets of 6-minutes-on, 24-minutes-off cycles. Data were taken during the first off-cycle from steady state and during the last off-cycle after the cycling pattern had been established. A final on-cycle was then initiated during which data were taken. This last on-cycle was generally allowed to continue until steady-state performance had been achieved instead of being terminated after six minutes of operation.

TEST DATA

Test conditions and pre-cycling steady-state data are summarized in Table 1. Transient capacity, power, and efficiency data are shown in Figures 1 through 3. In all cases the data are shown normalized by division by the steady-state value of the plotted quantity. In these figures LQVOL high or low refers to the liquid line volume corresponding to system refrigerant charges of approximately eight pounds and six pounds. The ACCU column indicates whether the accumulator was in the system or out. The AFTER column refers to the time period immediately preceeding the plotted data, either a 24-minute off-period (24 off), a six-minute on (6 on), or steady-state operation (SS). The MIGR column indicates whether off-cycle refrigerant migration was allowed or was prevented by shutting a pneumatically operated ball valve. In the past the observation was made (Mulroy and Didion 1985) that, for units allowing migration of refrigerant during the off-cycle and which have accumulators, the primary source of cyclic performance loss after the first minute of operation is the result of refrigerant being trapped in the accumulator. The unit will not reach steady state until the accumulator level has been reduced to its steady-state value, and until that time it will operate at a reduced efficiency and capacity proportional to the amount it is effectively "undercharged" by the amount of refrigerant held in the accumulator above the steady-state value.

In Figure 1, the cooling capacity data can be seen to be consistent with this observation. The configuration with the high charge, migration, and an accumulator displayed the worst performance. Reduction of the charge by eliminating a flowmeter, several valves, and a bypass circuit used with the flowmeter resulted in a clear improvement in performance. Here less charge resulted in less refrigerant going into the accumulator and, hence, less time to empty the accumulator and return to steady state. Eliminating the accumulator or preventing migration by use of a pneumatically operated ball valve, which simulated a thermal expansion valve without a bleed port, were found to give substantially similar results with migration prevention performing slightly better.

The on-cycle instantaneous heating capacities shown in Figure 1 differ from the cooling data in three significant ways.

First, although it does not show clearly in Figure 1, the initial value is slightly positive instead of negative as a result of fan power adding to capacity in the heating mode.

Second, the cyclic loss is much greater than in cooling. An explanation for this, for the refrigerant migration with accumulator cases, would be that more refrigerant will migrate in heating as a result of the greater temperature difference between the indoor test room and the outdoor ambient temperatures and that the portion of the accumulator return rate that is a function of heat gain to the accumulator from its surrounding air will be less because, in heating, the saturated suction temperature will be closer to ambient than in cooling.

Third, for those tests with migration, the higher charge gave better performance than the lower charge, results opposite to cooling and to expectations. Examination of data recorded during these tests but not included in this report indicate that this was a result of overfilling the accumulator. Thirty-four seconds after start-up, the higher charge test had a higher suction pressure (33.7 psig vs. 26.5 psig) but a much lower suction temperature (16.1 F vs. 41.4 F) than the lower charge test, indicating flooding into the compressor through the compressor suction line leaving the accumulator. After this rapid return had taken place, the amount the accumulator would be holding for slow return would be a smaller percentage of the total charge and, hence, a smaller degradation for the high charge case. In either case steady state would only be reached when the accumulator became empty (about one-half hour after start-up). This time would be about the same for the two cases, since the amount the accumulator would hold and the time to return it would be unchanged.

That flooding did not occur in the cooling mode indicates that greater migration takes place in the heating mode. In Mulroy and Didion (1985) it was found that, at the 82 F cyclic cooling test point for this unit, 80% of the refrigerant was on the low side at the end of a 24-minute off-cycle. It was calculated for a 47 F heating condition that if all the liquid refrigerant in the system migrated to the low side during the off-cycle, this would result in 91% of the refrigerant being on the low side.

The power consumption associated with the capacities of Figure 1 is shown in Figure 2. In all cases there is an initial surge that is over in approximately 30 seconds. After that time, the power consumption of the two cases with very low cyclic capacity loss (i.e., either no accumulator or no migration) quickly reaches the steady-state value. The cases with high cyclic capacity loss go to a lower power level than steady state and then rise to their steady-state value achieving this level more quickly than they did capacity.

The data of Figure 1 were divided by those of Figure 2 to give the instantaneous efficiency curves shown in Figure 3. The efficiency curves for the two low cyclic capacity loss cases are substantially the same as their capacity curves in Figure 1, since the power consumption values for these cases are at nearly their steady-state values. The high cyclic loss efficiency curves are somewhat higher than their capacity curves. This is because their coincident power is below the steady-state value. The high cyclic loss efficiency curves are well below the efficiency curves for the low cyclic loss cases.

The capacity recovered during the "off" portion of the cycle with continuous indoor fan operation is shown in Figure 4. In this case the four cooling configurations tested can be seen to give nearly the same performance as they fall from their initial value to a negative (heating instead of cooling) value equivalent to the heat imparted to the air by the indoor fan.

The off-cycle heating capacities in Figure 4 differ from the comparable cooling curves primarily in approaching a positive rather than a negative value as a result of fan energy being additive to heating and subtractive from cooling. Additionally, a dip can be observed in the cases with migration caused by boiling of the liquid refrigerant in the condenser as migration takes place as described in Murphy and Goldschmidt (1979).

DATA ANALYSIS

The test data of Figures 1, 2, and 4 are instantaneous values. To have relevance to a complete cycle, the data of Figures 1 and 2 must be integrated from cut-on to various cut-off times with some assumptions made as to what portion of the off-cycle capacity (Figure 4) and its associated power to add in as recoverable. The cyclic efficiency can then be calculated as the total capacity produced over the cycle divided by the total energy input, ${}_0\int^t (Q/Q_{ss})dt/\ {}_0\int^t (P/P_{ss}) = ({}_0\int^t Qdt/{}_0\int^t Pdt)/COP_{ss}$. This is not equal to the average of the instantaneous efficiency shown in Figure 3, $1/t\ {}_0\int^t((Q/P)/(Q_{ss}/P_{ss}))dt$.

The test data of Figures 1, 2, and 4 were analyzed by trapezoidal point integration for simulated cycles under three assumed operational modes: no off-cycle capacity recovery, off-cycle capacity recovery by fan delay until the recoverable capacity divided by the fan power was less than the steady-state efficiency, and off-cycle capacity recovery without penalty of fan power.

In all cases the off-cycle power to the control circuit and to the crankcase heater was omitted from the cyclic efficiency. This assumption eliminates length of off-cycle as a significant variable, assuming a typical minimum off-cycle of around five minutes for equipment reliability considerations, making cyclic efficiency a function of on-cycle length only.

The first approach, no off-cycle capacity recovery, is plotted in Figures 5 through 7.

The quantity plotted in Figure 5, $({}_0\int^t Q/Q_{ss}dt)/t$, is the average capacity from the beginning of an on-cycle. Two observations that can be made of the average capacity in comparison to the instantaneous capacity are (1) that it is a smoother curve because of the desensitizing to any one reading that is a natural consequence of the averaging process and (2) that it is lower because the average capacity includes the points earlier in the cycle when performance was poorer.

The average power plotted in Figure 6, $({}_0\int^t P/P_{ss}dt)/t$, can be seen to be nearer unity than the instantaneous power plotted in Figure 2, particularly for the cases with the best cyclic performance. This a result of the instantaneous power surge on start-up compensating for the post-start-up power drop occurring during periods of low capacity.

The same observations can be made about the average efficiency curves, Figure 7, as for the average capacities of Figure 5. That is, they are smoother and lower than the instantaneous efficiency curves.

It is clear that this approach always will result, irrespective of cycle length, in capacity and efficiency much less than steady state. In the real world, this case would correspond to a unit installed in an uninsulated closet, attic, or crawl, space which tended to lose any residual capacity stored in the coil mass during the off-cycle by heat transfer to the outdoor ambient.

The next approach to be considered is to recover the capacity stored in the coil mass by continuing to run the indoor fan. This is the most popular short-cycling device control strategy. Since the object of short cycling is to conserve energy, it was assumed that the off-cycle fan operation would be terminated when the off-cycle capacity divided by the fan power was less than or equal to the steady-state efficiency. Continued running beyond this point would result in degrading instead of improving the cyclic efficiency in comparison to the steady-state value. It should be noted that in cases where there is a latent (humidity) load, this fan delay will result in reevaporation of condensed water with associated conversion of latent to sensible cooling and a consequent failure to adequately dehumidify. Latent capacity was previously discussed in the section on test procedure.

The average capacity for this control strategy was calculated by integrating the on-cycle capacity, $\int_0^t Q/Q_{ss}dt$, adding to it the capacity that could be recovered if the unit were turned off at time t, Q_{R1}, and then dividing by the cycling on-time, t. The off-cycle recoverable capacity, Q_{R1}, was found by finding, by interpolation, the time, t1, in the appropriate off-cycle, as presented in Figure 4, at which the off-cycle capacity corresponded to the capacity at the end of the on-cycle, t, and then integrating the off-cycle from time t1 to that time, t2, at which the off-cycle capacity was equal to the product of fan power and steady-state efficiency. The average power was similarly calculated assuming constant fan power as $(\int_0^t Pdt + (t2 - t1)P_{FAN})/ tP_{ss}$. The efficiency was calculated as before as integrated cyclic capacity divided by the integrated cyclic power.

The results of this second set of calculations are shown in Figures 8, 9, and 10 to exhibit substantially better performance than the previous case but to still be inferior to the steady-state performance level.

The final calculation procedure was to assume that the off-cycle capacity could be recovered without fan operation; that is, the off-cycle temperature difference will be preserved in the insulated unit cabinet and will, with cyclic fan operation, be recovered at the start of the next cycle. Extensive research by the Air Conditioning and Refrigeration Institute (1984) has found that cyclic fan operation tests according to the Department of Energy test procedure (1979) can be closely simulated by continuous fan tests in which two minutes of the off-cycle capacity (plus fan energy in cooling, minus fan energy in heating) are added to the six-minute on-cycle and then divided by the on-cycle power. As can be seen in Figure 4, this two-minute period of continuous fan operation includes substantially all of the recoverable off-cycle capacity. For test times other than six minutes "on," integration was terminated on the off-cycle curve at the same data point as was used when the on-cycle capacity after six minutes set the starting point for integration with the integration end point two minutes thereafter. The total capacity resulting from these assumptions is shown in Figure 11, where the off-cycle recoverable capacity is referred to as Q_{R2}. The power is that of Figure 6; the cyclic efficiency is shown in Figure 12.

The level of performance with this control strategy is always better than the previous two cases, indicating that cyclic fan is more efficient than fan delay. That is, almost all available off-cycle capacity is still harvested with cyclic fan but without a fan power penalty. Finally, the level of performance with this best strategy is still always below the steady-state value.

It can be observed in Figure 12, for those tests that have off-cycle refrigerant migration, there is an efficiency peak approximately .6 minutes after start-up, followed by a minimum approximately 1.1 minutes after start-up and a recovery to the early peak approximately 3.7 minutes after start-up. Although this dip is small, approximately 3% below the early peak, the question arises whether it would be worthwhile to add a device to prohibit on-times between .6 minutes and 3.7 minutes. The answer to this is that under normal thermostat control, cycles as short as this never occur, so this question is moot. This is because minimum on-cycle lengths under normal thermostat control are set by the need to satisfy a thermostat differential of approximately 2 F (1.1°C). As percent run times approach 0, on- times approach a finite value and off-times approach infinity. For a conventional parabolic thermostat model (Parken et al. 1985) the on-time is given by:

$$t_{on} = \frac{1}{4\ N_{max}(1 - \Gamma)}$$

<u>where</u>

t_{on} = on-cycle length, minutes

N = cycles per hour at 50% run time

Γ = fractional run-time

With a run time of 0 and N_{max} values of 2 to 3 cycles per hour, typically used for air conditioners and heat pumps, values of the minimum on-time are between 5 minutes and 7.5 minutes, both well past the inflection point in the efficiency curves. Actual on-times would be expected to be longer than this, since one of the primary simplifications of this thermostat model is that there is no cyclic capacity degradation.

Table 1 lists the cyclic degradation factors, C_D, as defined in ASHRAE (1983) with the exceptions that capacity and power were integrated according to the three schemes discussed in this section and that the off-cycle control circuit and crankcase heater power were omitted.

CONCLUSIONS

For all tests, no integrated cyclic capacity, including the capacity that could have been recovered during the consequent off-period, was observed, which was equal to or greater than the steady-state value. Similarly, no cyclic efficiency was observed equal to or greater than the steady-state efficiency. It was also observed that there is no short-cycling device control strategy that would increase the efficiency of a residential air conditioner or heat pump, similar in design to the systems tested, beyond that provided by a conventional thermostat. In fact, such-short cycling devices would cause a loss of efficiency in meeting the imposed building load. This loss, which would occur in applying such a device, was observed to be greater for units of low cyclic efficiency than those of the highest efficiency.

It was further observed that efficiency was greater as calculated by the procedure of ARI 210/240-84, which simulates cyclic fan performance from continuous fan data, than was the efficiency calculated assuming a fan delay control strategy. This was because it is more efficient to harvest the off-cycle recoverable capacity as part of the next cycle than it is to expend fan power and heat to recover this capacity at the end of a cycle. Because of this decreased efficiency and because of loss of latent capacity, it can be concluded that fan delay is a counterproductive control strategy for air conditioners and heat pumps with the indoor air handler and coil within the conditioned space.

If the indoor air-handling unit and coil are outside the conditioned space, fan delay would be expected to recover heat that would otherwise be lost.

Additional observations were that cyclic losses are very low for units that do not allow off-cycle migration or do not have accumulators. Units with accumulators that allow off-cycle migration have increasing cyclic losses with increasing charge until migration on start-up results in overfilling the accumulator.

NOMENCLATURE

ACCU in figures, indicates presence or absence of accumulator

AFTER in figures, indicates plotted data was preceded by a 24-minute-off (24 off), 6-minute-on (6 on), or steady-state (ss) period of operation.

COP = coefficient of performance

LQVOL in figures, indicates high or low liquid line volume for a total system charge of either 8 pounds or 6 pounds of R22.

MIGR in figures, indicates whether off-cycle refrigerant migration was allowed or prevented by a pneumatically operated valve in the liquid line.

N = cycles per hour at 50% run time

P = total electric power draw, watts

P_{FAN} = fan power, watts

Q = total cooling (sensible plus latent) or heating capacity, Btu/h

Q_{R1} = cooling or heating capacity recoverable during an off-cycle by fan delay, Btu/cycle

Q_{R2} = cooling or heating capacity recoverable during a continuous fan off-cycle that, when added to the on-cycle, would result in a total capacity equal to that which would have been measured had fan operation been cyclic, Btu/cycle

SS = steady state

t = time

t_{on} = on-cycle length, minutes

Γ = fractional run time

REFERENCES

Mulroy, W.J., and Didion, D.A. 1985. "Refrigerant migration in a split-unit air conditioner." ASHRAE Transactions, Vol. 91, Part 1.

Deparment of Energy, Office of Conservation and Solar Energy. 1979. "Test procedures for central air conditioners including heat pumps." Federal Register, Thursday, December 27, 1979, Part III.

ASHRAE. 1983. ANSI/ASHRAE Standard 116-1983, "Methods of testing for seasonal efficiency of unitary air-conditioners and heat pumps." Atlanta: American Society of Heating, Refrigerating and Air-Conditioning Engineers, Inc.

Murphy, W.E., and Goldschmidt, V.W. 1979. "Qualitative interpretation of transient performance." Herrick Laboratories, HL 7903, Purdue University, Lafayette, Indiana.

Air Conditioning and Refrigeration Institute. 1984. ARI Standard 210/240-1984, "Standard for unitary air-conditioning and air-source heat pump equipment." Arlington, Virginia.

Parken, W.H. Didion, D.A.; Wojciechowski, P.H.; and Chern, L.; 1985. "Field performance of three residential heat pumps in the cooling mode." NBSIR 85-3107. Gaithersburg, Maryland: National Bureau of Standards.

ACKNOWLEDGMENT

The research reported herein has been supported by the Office of Conservation and Renewable Energy of the U.S. Department of Energy.

TABLE 1
Summarized Steady-State Data and C_D Values

TEST NO.	MODE	SYSTEM CHARGE LBS OF R22	ACCUMULATOR	OFF-CYCLE MIGRATION	STEADY-STATE CAPACITY, Btu/hr	STEADY-STATE TOTAL POWER, W	INDOOR FAN POWER, W	INDOOR AIR TEMP, F	OUTDOOR AIR TEMP, F	C_{D1}	C_{D2}	C_{D3}
5	Cooling	8	in	yes	31,110	3859	512	80.2	82.3	.344	.268	.221
9	Cooling	6	out	yes	31,610	4038	507	79.7	82.4	.198	.120	.067
7	Cooling	6	in	yes	31,710	4031	506	79.8	82.3	.264	.183	.129
8	Cooling	6	in	no	31,670	4022	505	79.8	82.1	.185	.121	.075
1	Heating	8	in	yes	32,510	3605	476	69.8	47.0	.466	.392	.375
2	Heating	8	in	no	32,930	3630	481	69.9	47.0	.252	.155	.120
3	Heating	6	in	yes	33,770	3633	478	70.1	47.0	.492	.429	.414
4	Heating	6	in	no	32,900	3616	479	70.1	46.9	.256	.166	.134

C_{D1} was calculated with no off-cycle capacity recovered.

C_{D2} includes off-cycle capacity and power recovered by fan delay.

C_{D3} follows the calculation procedure of ARI 210/240-84 with off-cycle power omitted.

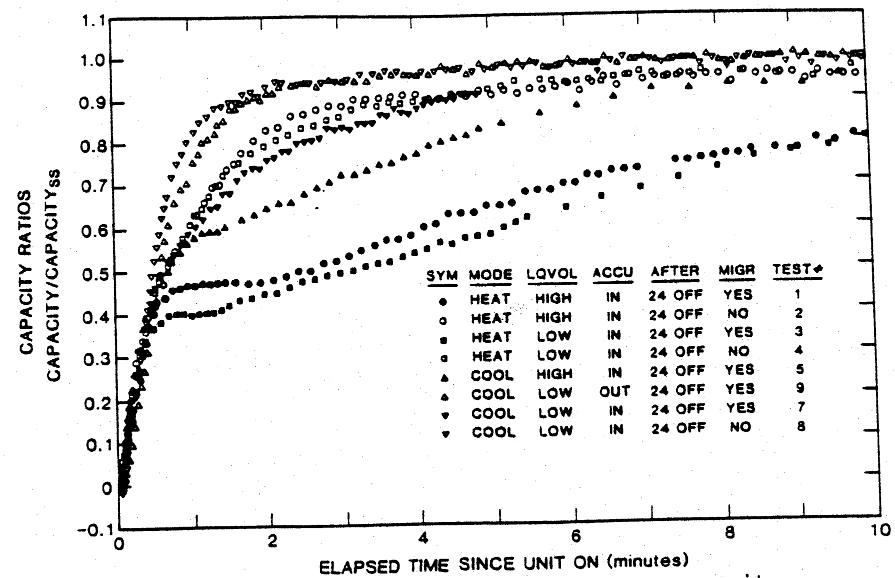

Figure 1. On-cycle instantaneous capacity

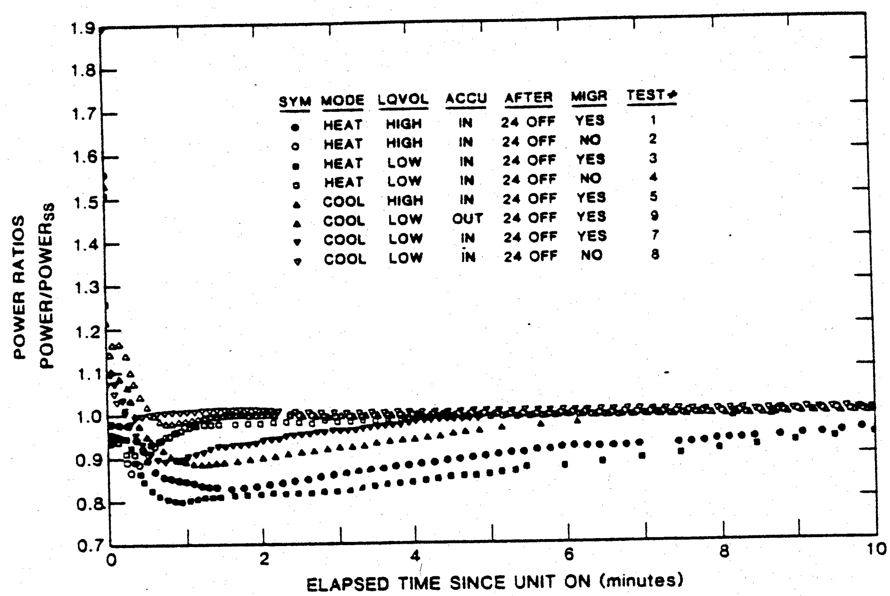

Figure 2. On-cycle instantaneous power

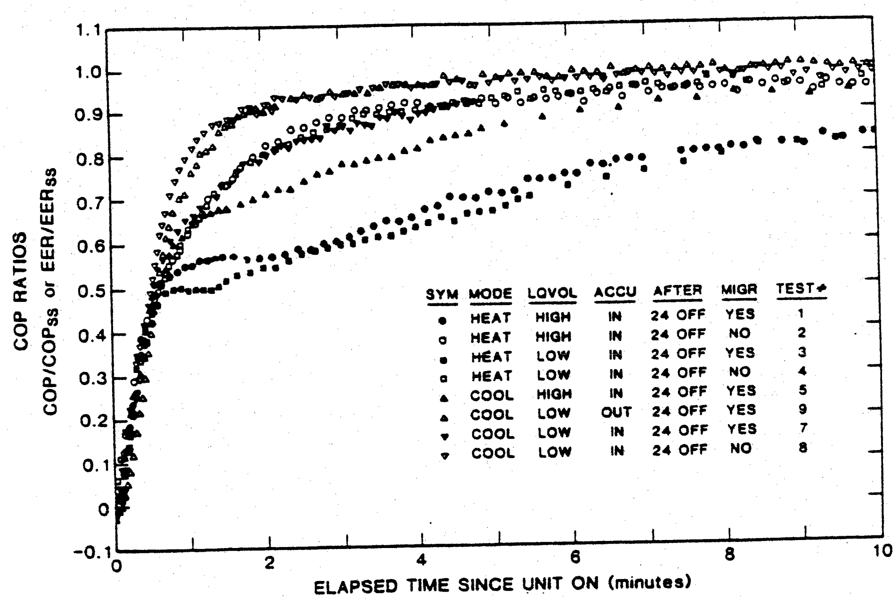

Figure 3. Instantaneous efficiency

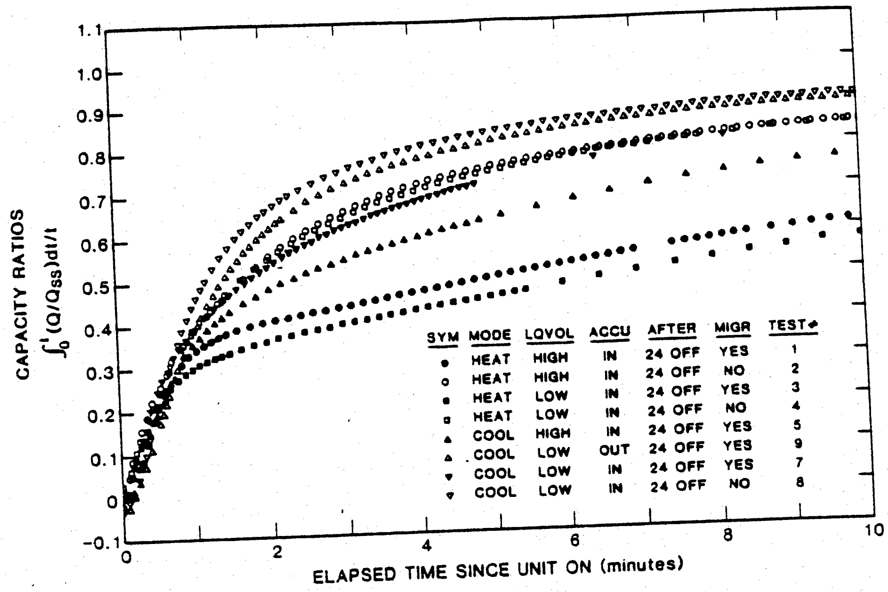

Figure 4. Off-cycle instantaneous capacity

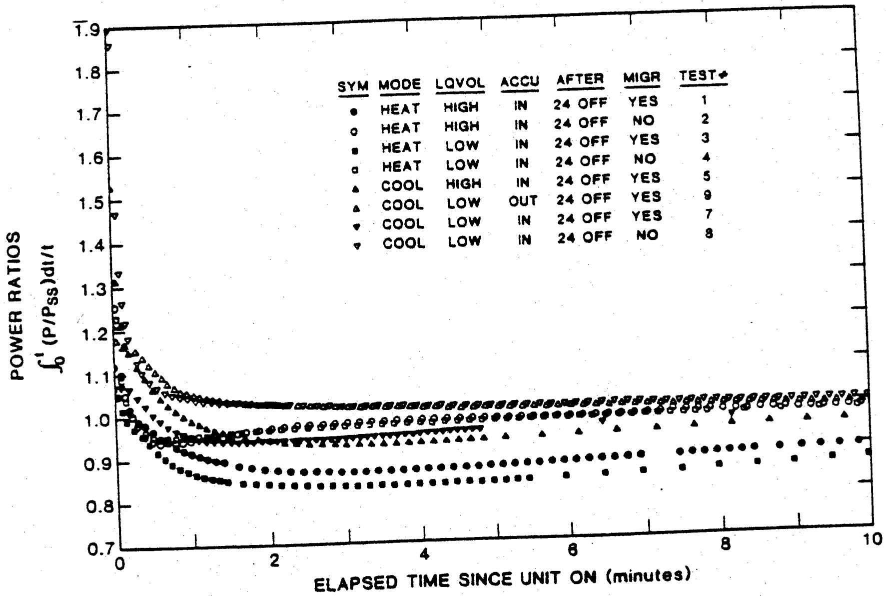

Figure 5. Average capacity from cut-on

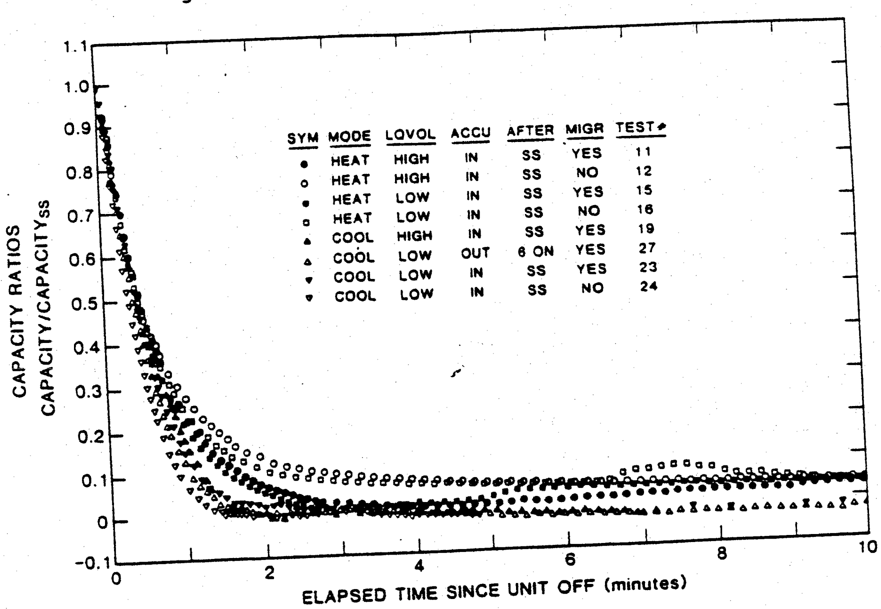

Figure 6. Average power consumption from cut-on

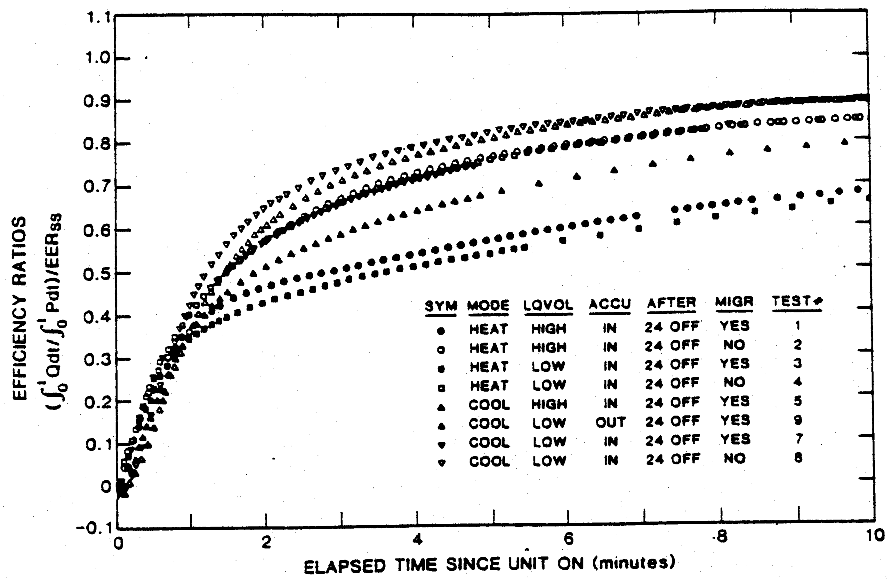

Figure 7. Cyclic efficiency without off-cycle capacity recovery

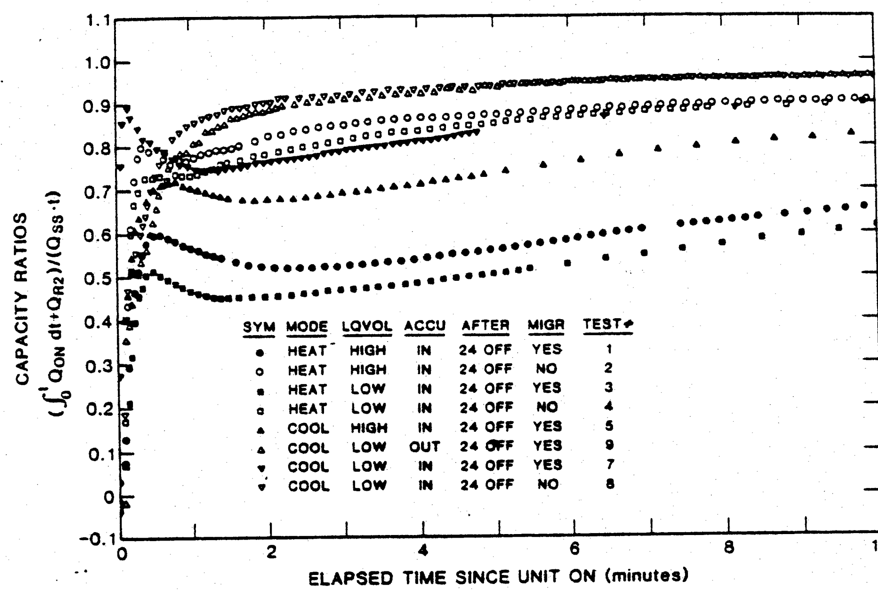

Figure 8. Average capacity from cut-on plus off-cycle capacity recoverable by fan delay

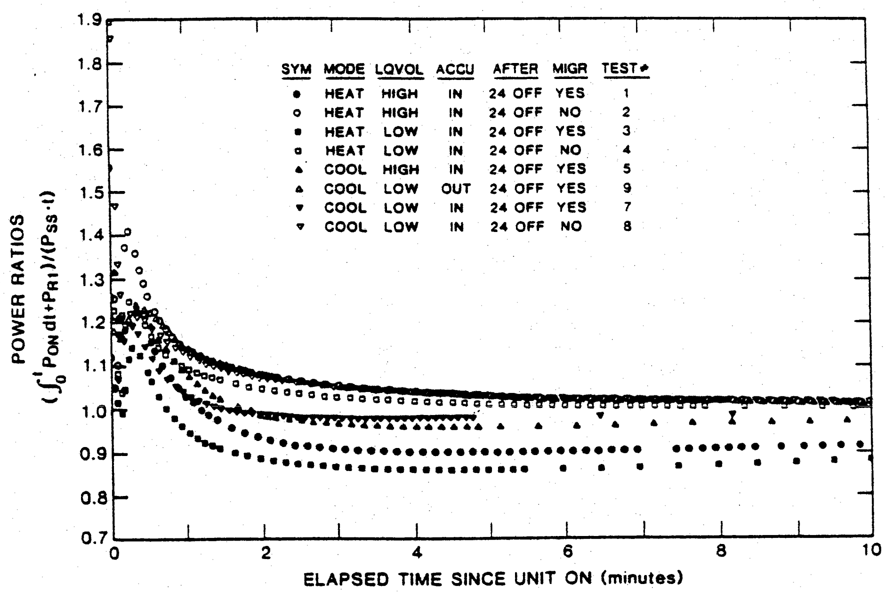

Figure 9. Average power from cut-on plus fan power required to recover off-cycle capacity by fan delay

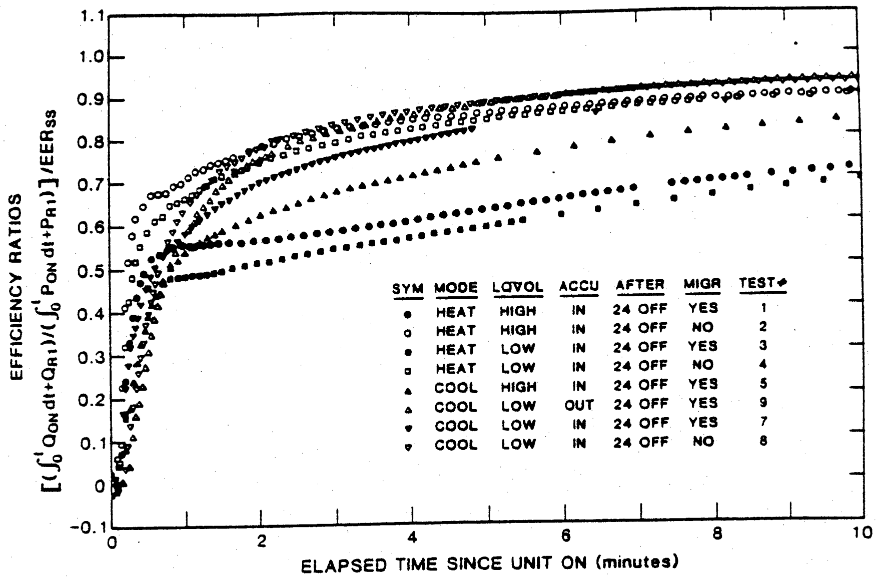

Figure 10. Cyclic efficiency assuming off-cycle recovery by fan delay

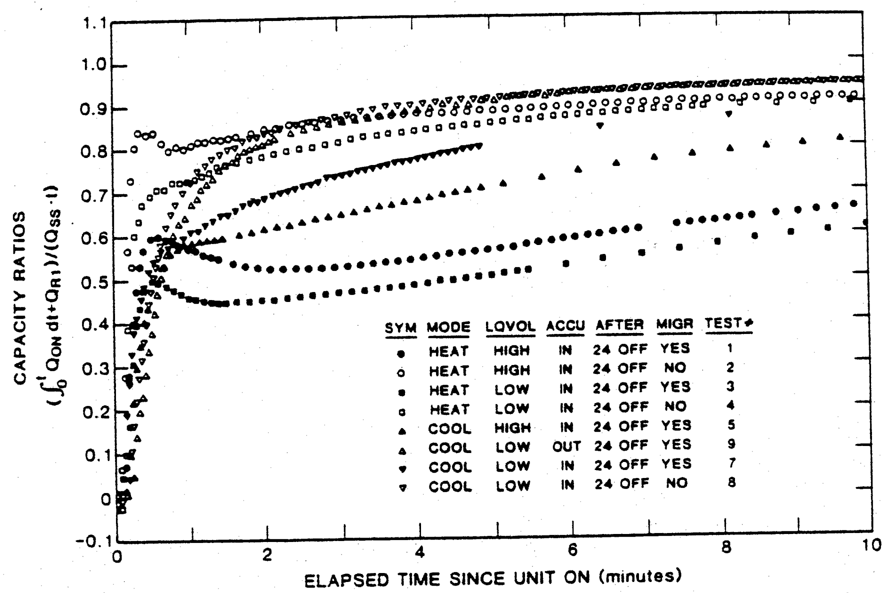

Figure 11. Average capacity from cut on assuming cyclic fan operation and off-cycle capacity recovery

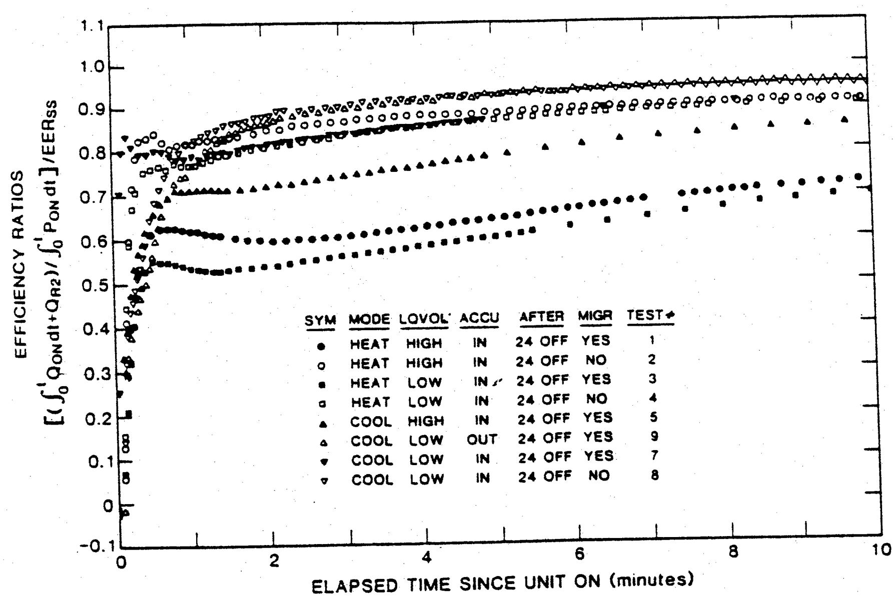

Figure 12. Cyclic efficiency assuming cyclic fan operation and off-cycle capacity recovery